AJNR

Congenital porencephaly: MR features and relationship to hippocampal sclerosis.

S S Ho, R I Kuzniecky, F Gilliam, E Faught, M Bebin and R Morawetz

Congenital Porencephaly: MR Features and Relationship to Hippocampal Sclerosis

Susan S. Ho, Ruben I. Kuzniecky, Frank Gilliam, Edward Faught, Martina Bebin, and Richard Morawetz

PURPOSE: We determined the frequency of amygdalar-hippocampal atrophy in patients with congenital porencephaly-related seizure disorders to ascertain whether specific MR features of the porencephaly correlate with amygdalar-hippocampal atrophy and epilepsy.

METHODS: We studied brain MR images of 22 patients with congenital porencephaly and measured the volume of the amygdala, the hippocampal formation, and the porencephalic cyst. We then compared imaging features with seizure symptoms.

RESULTS: Porencephaly was unilateral in 20 patients and bilateral in two. Eighteen patients had cortical or subcortical cavitation and four had encephaloclastic changes (noncircumscribed parenchymal destruction associated with cystic components). The porencephaly was located in the middle cerebral artery territory in 12 patients, in the posterior cerebral artery in four, in the internal carotid artery in two, and in multiple vessels in four. The volume of the porencephalic cyst ranged from 1% to 32% of total intracranial volume (mean, 11%). Volumetry detected atrophy of the hippocampal formation in 21 cases (11 unilateral, 10 bilateral) and atrophy of the amygdala in 12 (nine unilateral, three bilateral). No correlation was found between size or location of the porencephaly and degree of hippocampal atrophy. Seizure symptoms correlated with mesial temporal origin but not with cyst location.

CONCLUSION: Amygdalar-hippocampal atrophy often coexists with congenital porencephaly (95%), and the atrophy may be bilateral despite unilateral cysts. Hippocampal structures should be carefully assessed in patients with porencephaly-related seizures.

Radiologic features in congenital porencephaly-related seizure disorders have not been well studied. The majority of previous studies have been based on computed tomography (CT) and thus may not provide optimal imaging information of relevance to patients with epilepsy associated with congenital porencephaly. Moreover, there has been much diversity among previous studies in regard to the relationship between radiologic features and seizure characteristics (1–4). These authors disagreed on whether lesion morphology on CT scans correlated with the frequency of seizures, although seizure symptomatology was not specifically examined. A recent study using magnetic resonance (MR)-based volumetry described the association of mesial temporal sclerosis with a variety of extratemporal lesions, including a few cases of porencephaly (5), but the authors' method of case inclusion was unclear, and the prevalence of atrophy in patients with porencephaly-related seizure disorders cannot be ascertained from this study. The coexistence of mesial temporal sclerosis with extrahippocampal lesions has been referred to as "dual pathology." Study of the interrelationship among dual pathology, porencephalic lesion morphology, and epilepsy might provide a clue to the neurobiology of epilepsy in patients with congenital porencephaly.

MR-based volumetry is the most sensitive method for the presurgical detection of mesial temporal sclerosis (6–8). Inclusion of a normalization process allows the definition of absolute hippocampal volumes and can enable the detection of unsuspected bilateral hippocampal volume loss (9, 10). We therefore used this quantitative technique to assess the frequency of amygdalar-hippocampal atrophy in a homogeneous population of patients with congenital porencephaly and intractable seizures. We correlated porencephalic lesion location and morphology with amygdalar-hippocampal abnormalities and seizure symptomatology to determine whether specific radiologic features are associated with seizure manifestation.

Methods

Patients were recruited from a center for epilepsy referral. In all cases, porencephaly was detected during routine MR investigation of intractable seizures. Patients with acquired cystic lesions (ie, after trauma, tumor resection, or infection) or cystic developmental malformations (eg, schizencephaly) were excluded from the study. The patients had detailed neurologic evaluation and routine electroencephalographic (EEG) studies using the international 10–20 system. Thirteen patients had long-term video EEG monitoring with scalp electrodes. One patient had intracranial EEG monitoring with subdural electrodes.

MR Imaging

All subjects were imaged in a 1.5-T magnet using a standardized protocol. Sagittal T1- and coronal T2-weighted spin-echo fluid-attenuated inversion recovery (FLAIR) sequences were obtained with parameters of 8000/180/1 (repetition time/echo time/excitations) and an inversion time (TI) of 2100. Inversion recovery sequences were acquired with parameters of 1200/20 and a TI of 300. For volumetric studies, a three-dimensional spoiled gradient-echo (20/6.2/1) sequence was used with a 23-cm field of view, a flip angle of 28°, and a matrix size of 218 × 256 to acquire images in the coronal plane perpendicular to the long axis of the hippocampus, and were then formatted to 1.5-mm contiguous coronal sections without gaps.

MR Visual Analysis

The MR images were analyzed for the presence of porencephalic changes, including cavitation (well-circumscribed cystic appearance), encephaloclastic changes (poorly circumscribed areas of parenchymal destruction associated with cystic components), and ventricular enlargement. The extent of involvement of the thickness of the hemisphere was described as either cortical or subcortical. The arterial supply territory of the porencephalic lesion was determined according to Patten (11). In addition, the MR images were evaluated qualitatively for the presence of hippocampal atrophy and signal alterations indicative of mesial temporal sclerosis (signal hypointensity on T1-weighted inversion recovery images and signal hyperintensity on FLAIR sequences) according to previously validated diagnostic criteria (12).

MR Volumetric Analysis

The images were transferred to a Silicon Graphics Indigo workstation (Mountain View, Calif) for volumetric measurement using a software program developed in a laboratory of the University of Alabama. The regions of interest (ROIs) were outlined by the same interpreter using the manual contouring function, and the section volume was calculated automatically by the computer program. Anatomic guidelines for outlining the amygdala and hippocampal formation were consistent with the protocol described by Watson et al (13). Using this protocol, the rater has an intraobserver test-retest coefficient of variation under 2%. Interrater testing showed no statistical difference in our laboratory.

Volumes of the amygdala and hippocampal formation were obtained for each patient and compared with values obtained from healthy control subjects according to age criteria. The patient group consisted of 12 male and 10 female subjects with a mean age of 33 years (age range, 3 to 54 years; median, 34 years). The control subjects were grouped by age as follows: 25 to 38 years (n = 10; seven men, three women), 9 to 15 years (n = 4, three boys, one girl), and 3 to 6 years (n = 4, two boys, two girls). The age criteria in the control groups were chosen to match the age distribution in the patient population. The hippocampal and amygdalar volumes in the patients were normal-ized using data from control subjects of similar ages to minimize variability in volumes due to different ages and sizes of the patients. We used a previously validated method for normalization of amygdalar and hippocampal volumes (9, 10, 14) as follows:

1) $$NV = OV - Grad(TCV_i - TCV_{mean})$$

where NV is the normalized hippocampal or amygdalar volume, OV is the observed hippocampal or amygdalar volume, Grad is the regression gradient or slope of the regression line of hippocampal or amygdalar volume regressed on total intracranial volume for the control group, TCV_i is the cranial volume for the individual subject, and TCV_{mean} is the mean intracranial volume for the group of control subjects. The cranial volume was estimated from area measurements on 14 sagittal 5-mm-thick sections equally spaced throughout the cerebrum, using the same volume analysis program as that for the hippocampal and amygdalar volume measurements.

Abnormal volumes were defined as 2 standard deviations (SD) below the mean for the normalized data of the control subjects. Side-to-side hippocampal symmetry was determined by subtracting left- from right-sided volumes (using corrected values). Only individuals in whom this right-minus-left difference fell between -0.1 and 0.3 cm^3 (inclusive) were considered to have symmetric hippocampi (8).

The volume of the porencephalic cyst was determined by using the same volume analysis program. On sagittal 5-mm-thick sections without gaps, we outlined an ROI around the cyst and adjacent ventricle. The cyst-ventricle was selected as the ROI because, in some cases, the boundary between cyst and ventricle cannot be clearly identified. The volume of the cyst-ventricle was calculated by summing ROIs in contiguous sections and multiplying by section thickness. From here on, the cyst-ventricle volume is simply referred to as cyst volume. We defined cyst ratio as cyst volume divided by total intracranial volume (TCV_i).

Statistical Analysis

We used Fisher's Exact Test to compare categorical data and an unpaired t test to compare the means of the two groups. Linear regression was used to test the correlation between hippocampal and cyst volumes. The significance level was set at $P < .05$.

Results

Clinical features of the 22 patients are listed in Table 1. Thirteen patients had a history of pre- or perinatal ischemic insult, 10 had intellectual impairment, and 19 had congenital hemiparesis associated with hemiatrophy. All patients had chronic epilepsy at the time of the study. Seventeen patients had complex partial seizures, three had sensorimotor simple partial seizures, and two had generalized tonicoclonic seizures with no history to suggest a focal onset.

Surface interictal EEG showed a temporal epileptic focus in 10 patients, bitemporal discharges in one, and extratemporal epileptiform abnormalities in five; EEG was nonlocating in the others. Of the 13 patients who underwent long-term video EEG monitoring with scalp electrodes, four had ictal discharges indicative of temporal location. One patient had intracranial EEG monitoring with confirmation of temporal location.

TABLE 1: Clinical findings and qualitative MR features of porencephaly

Patient	Age, y/Sex	Seizure Symptoms	MR Features of Porencephalic Lesion			
			Location	Pattern	Cyst Ratio*	Arterial territory
1	34/M	CPS	L frontoparietotemporal, posterior limb of internal capsule and adjacent white matter	Cortical-subcortical cavitation	0.2	ICA
2	30/F	CPS	L temporoparietooccipital	Cortical-subcortical cavitation	0.02	PCA
3	15/M	CPS	R parietooccipital, inferotemporal and thalamus	Cortical-subcortical cavitation	0.16	PCA
4	39/M	CPS	R frontoparietal and superior temporal	Cortical-subcortical cavitation	0.1	MCA
5	42/M	GTCS	R parietooccipital	Subcortical cavitation	0.03	MCA (deep branch)
6	52/F	SPS	Bilateral parietooccipital and posteroinferior temporal	Ventricular dilatation and encephaloclastic changes	No cyst	Multivessel (distal)
7	32/M	CPS	R basal ganglia	Ventricular dilatation and encephaloclastic changes	No cyst	MCA (deep branch)
8	52/M	CPS	R anterior frontal, parietotemporal, and posterior limb of internal capsule	Cortical-subcortical cavitation	0.05	ICA
9	31/M	CPS	R frontoparietal and superior temporal	Cortical-subcortical cavitation	0.13	MCA
10	49/F	CPS	R parietotemporal	Ventricular dilatation and encephaloclastic changes	No cyst	MCA
11	33/F	SPS	L basal ganglia, centrum semiovale	Cortical-subcortical cavitation	0.05	MCA (deep branch)
12	40/F	SPS	L parietotemporal, basal ganglia	Cortical-subcortical cavitation	0.02	MCA (deep branch)
13	24/M	CPS	R frontoparietotemporal	Cortical-subcortical cavitation	0.28	MCA
14	54/M	CPS	Bilateral frontoparietal and temporal	Cortical-subcortical cavitation	0.32	Bilateral PCA
15	22/M	CPS	R anterior and mesial frontal, parietal, and temporal	Cortical-subcortical cavitation	0.2	ACA, MCA, and PCA
16	3/F	GTCS	L frontocentroparietal and temporal	Cortical-subcortical cavitation	0.18	MCA and PCA
17	35/M	CPS	R frontal and temporal	Cortical-subcortical cavitation	0.02	MCA
18	30/F	CPS	R parietooccipital	Encephaloclastic changes	0.03	PCA
19	45/M	CPS	L parietotemporal	Cortical-subcortical cavitation	0.03	MCA
20	12/F	CPS	L parietooccipital and superior temporal	Cortical-subcortical cavitation	0.2	PCA and MCA
21	4/F	CPS	L parietal and superior temporal	Cortical-subcortical cavitation	0.01	MCA
22	44/F	CPS	L centroparietal	Subcortical cavitation	0.01	MCA (deep branch)

Note.—MCA indicates middle cerebral artery; PCA, posterior cerebral artery; ICA, internal carotid artery; ACA, anterior cerebral artery; CPS, complex partial seizures; SPS, simple partial seizures; and GTCS, generalized tonicoclonic seizures.

* Porencephalic cyst volume divided by total intracranial volume.

Qualitative MR Analysis

Twenty patients had unilateral and two had bilateral porencephalic changes (Fig 1). The abnormalities comprised cavitation changes in 18 cases (14 cortical-subcortical, two subcortical) and predominantly encephaloclastic changes in four. The porencephaly was located in the middle cerebral artery territory in 12 patients (Figs 2A and 3), in the posterior cerebral artery in four (Fig 4), in the internal carotid artery in two (Fig 5), and in multiple vessels in four (Fig 6). Hippocampal atrophy was visually detected in 17 of the 22 patients, and 13 patients had abnormal signal changes in the hippocampus, consisting of hyperintensity on FLAIR sequences and hypointensity on inversion recovery sequences, indicative of sclerosis. In two cases, a bilateral hippocampal abnormality was evident; one patient (case 17) had asymmetric bilateral hippocampal atrophy and the other (case 20) had symmetric hippocampal atrophy associated with bilateral T2 signal hyperintensity on the FLAIR sequence (Fig 6).

Quantitative MR-Based Volumetric Analysis

The mean (2 SD) normalized hippocampal and amygdalar volumes for the three control groups are given in Table 2. The normalized hippocampal and amygdalar volumes for the patient group are shown in Table 3. On the assumption that values less than 2 SD (95% confidence) below the mean for the control group were abnormal, volumetry detected hippocampal atrophy in 21 patients (11 unilateral, 10 bilateral) and amygdalar atrophy in 12 (nine unilateral, three bilateral). One patient had a normal amygdala and hippocampal formation at both volumetric measurement and visual assessment (Fig 3). Of the 10 patients with bilateral hippocampal atrophy, two had a right-minus-left volume difference that met the criteria of
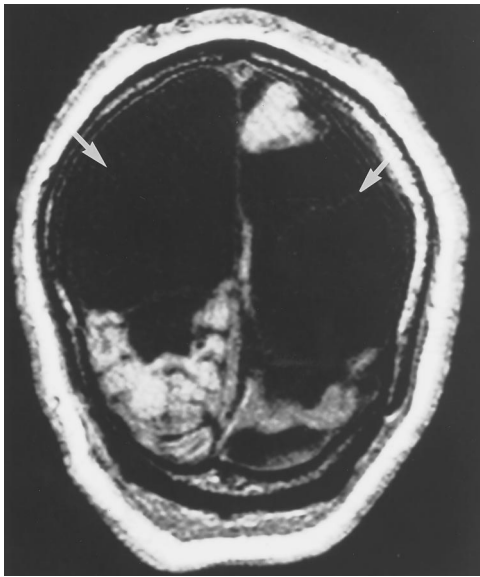
FIG 1. Case 14: patient with complex partial seizures and bitemporal interictal discharges on EEG. Volumetric T1-weighted MR image (20/6.2/1) in the coronal plane shows bilateral porencephalic cysts (*arrows*) in the posterior cerebral artery distribution.

bilateral, symmetric hippocampal atrophy (cases 7 and 20); the other eight patients had bilateral asymmetric hippocampal atrophy. Porencephalic cyst volume ranged from 1% to 32% of total intracranial volume (mean, 11%).

Data Analysis

Fisher's Exact Test showed no significant association between seizure symptoms and porencephalic lesion morphology (cortical or subcortical cavitation versus encephaloclastic changes). Nor was an association found between porencephalic cyst volume and seizure symptoms or between anatomic location of the porencephalic lesion (anterior circulation versus posterior circulation) and seizure symptoms. Linear regression did not reveal a significant correlation between cyst volume and seizure frequency.

Of the 21 patients with hippocampal atrophy, 17 (81%) had clinical manifestations of complex partial seizures, three had sensorimotor simple partial seizures, and one had generalized tonicoclonic seizures only. The one patient with normal hippocampal volumes had nocturnal generalized seizures that were subsequently controlled with antiepileptic medications. This patient had no evidence of temporal lobe seizure onset. No statistical correlation was found between seizure frequency and severity of hippocampal volume loss, nor was there a correlation between duration of epilepsy and degree of hippocampal atrophy.

In the patients with unilateral hippocampal atrophy, the side of atrophy was ipsilateral to the porencephaly in 10 of 11 cases (Fig 4); in the one patient in whom hippocampal atrophy was contralateral to the cyst (Fig 2), ictal EEG showed clear temporal onset ipsilateral to the atrophy. In the 10 patients with bilateral hippocampal atrophy, two also had bilateral porencephaly; in seven cases, the more severely atrophic hippocampal formation was ipsilateral to the porencephalic lesion, and in one case, the more severely atrophic hippocampal formation was contralateral to the porencephaly. There was no significant correlation between the volume of the porencephalic cyst and the severity of the hippocampal volume loss (correlation coefficient, $r = -0.21$, F = 0.84).

Surgical Results

Four patients (cases 1–3 and 22) underwent temporal lobe surgery and all had pathologic confirmation of mesial temporal sclerosis. Two patients were seizure-free at 18 months' follow-up (cases 1 and 2); the other two have also remained seizure-free since their surgery, but the follow-up periods were less than 6 months.

Discussion

Seizures are an important cause of morbidity in patients with congenital porencephaly. Correlation of the structural lesion with electroclinical findings may enable effective surgical treatment in patients with seizures refractory to medical therapy. Previous clinicoradiologic studies with CT have produced conflicting findings (1–4). Our findings suggest a lack of correlation between MR porencephalic lesion morphology and seizure manifestation; further, no correlation was found between porencephalic lesion location and seizure symptoms. A majority of the patients (17 of 22 cases) had typical temporal lobe seizure symptoms, comprising complex partial seizures of the psychomotor type, and the seizure symptoms did not correspond to the extratemporal location of the porencephalic cysts. Although five patients had seizure manifestation not suggestive of temporal origin, electroclinical correlation with the extratemporal location of the porencephalic cyst was possible in only two of the cases. There was no association between the vascular territory of the porencephalic lesion and the seizure symptoms. Furthermore, the size of the porencephaly did not correlate with seizure symptoms or seizure frequency.

Surprisingly, we found a high prevalence of coexisting amygdalar and hippocampal atrophy in this group of patients. Dual pathology has been reported previously by Cendes et al (5) in a heterogeneous group of patients with extratemporal lesional epilepsy, including a few patients with porencephaly; however, in contrast to their study, we found a much higher rate of coexisting hippocampal atrophy (95% versus 31%), and a high proportion of the patients had bilateral amygdalar-hippocampal involvement. Bilateral amygdalar-hippocampal atrophy was not reported in the study by Cendes et al, which did not include a process for volume normalization. In contrast to the lack of correlation between seizure symptoms and porencephalic location or morphology,
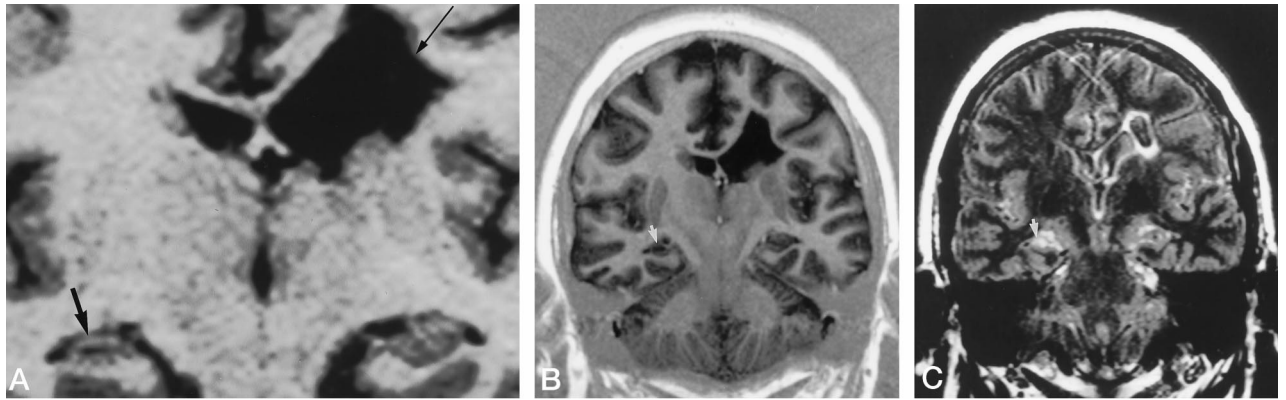
FIG 2.   Case 22: patient with intractable complex partial seizures of right temporal lobe origin.

A, Volumetric T1-weighted MR image (20/6.2/1) in the coronal plane shows a left subcortical porencephaly in the distribution of the deep branches of the left middle cerebral artery (*thin arrow*) with coexisting contralateral right hippocampal atrophy (*wide arrow*) (original magnification ×2).

B, Inversion recovery sequence (1200/20, TI = 300) shows a hypointense signal in the right hippocampus, indicative of sclerosis (*arrow*).

C, FLAIR sequence (8000/180, TI = 2100) shows a hyperintense signal (*arrow*) in the right hippocampus corresponding to the low signal in *B*.
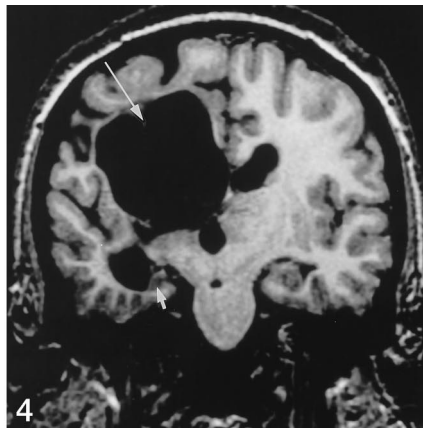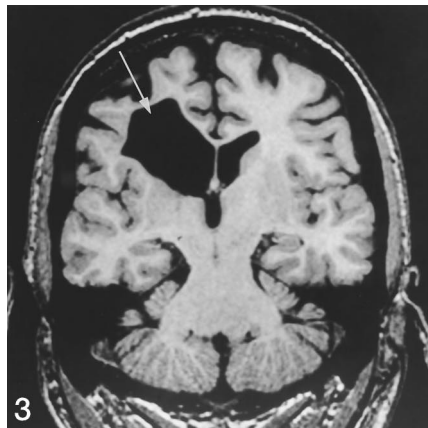

FIG 3.   Case 5: volumetric T1-weighted MR image (20/6.2) shows a porencephaly (*arrow*) without hippocampal atrophy in a deep branch of the right middle cerebral artery distribution.

FIG 4.   Case 3: patient with complex partial seizures of right temporal lobe origin. Volumetric T1-weighted MR image (20/6.2) in the coronal plane shows a right posterior cerebral artery distribution porencephaly (*long arrow*) and ipsilateral right hippocampal atrophy (*short arrow*). The porencephalic cyst extends from the right parietotemporal region to the occipital cortex and involves the calcarine fissure.
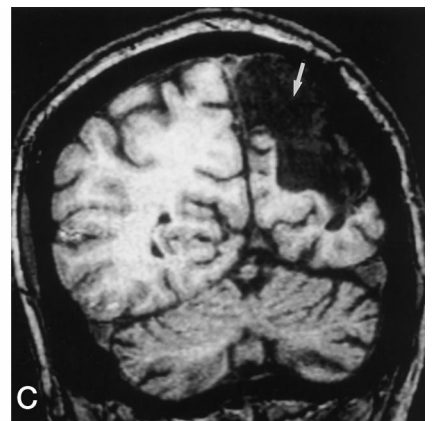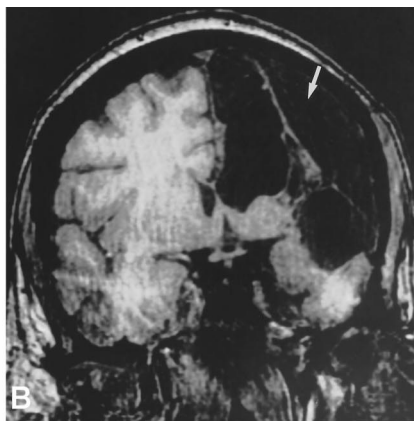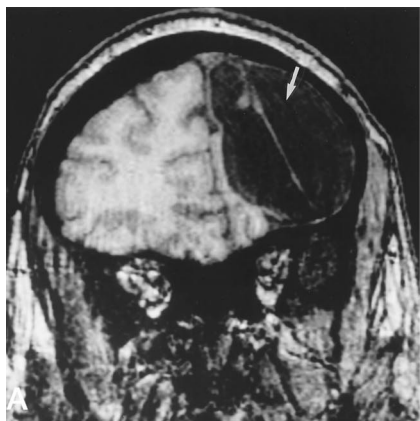

FIG 5.   Case 1. Noncontiguous volumetric T1-weighted MR images (20/6.2/1) in the coronal plane show a left porencephalic cyst in the distribution of the left internal carotid artery (*arrow*). This arterial territory is identifiable by involvement of the cortex supplied by the middle cerebral territory, as well as by involvement of the posterior limb of the internal capsule and the posterolateral white matter, which are supplied by the anterior choroidal artery.

there was good concordance between electroclinical evidence of temporal lobe seizure onset and presence of ipsilateral amygdalar-hippocampal atrophy. In one patient in whom the hippocampal atrophy was contralateral to the porencephaly (case 22), electroclini-

cal location accorded with the side of the hippocampal atrophy and not the porencephaly. This patient had confirmation of mesial temporal sclerosis at surgical pathologic examination and has been seizure free since temporal lobe surgery. There was no cor-
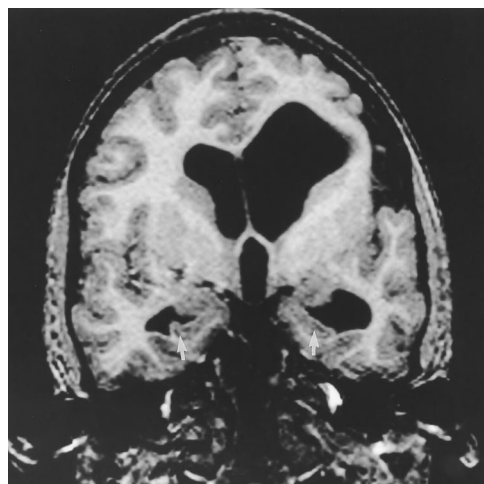
FIG 6.   Case 20: volumetric T1-weighted MR image (20/6.2/1) in the coronal plane shows a left porencephalic cyst in the distribution of the left posterior cerebral and distal left middle cerebral arteries. *Arrows* indicate coexisting bilateral symmetric hippocampal atrophy.

relation between the severity of hippocampal volume loss and attributes of the porencephaly, including cyst volume, anatomic location, and vascular distribution.

The high frequency of dual pathology in this group of patients is striking. The exact mechanism for the amygdalar-hippocampal atrophy is unknown. Repeated seizures from electrical kindling have been shown to produce hippocampal cell loss in rats (15). The quantitative detection of amygdalar-hippocampal atrophy in almost all the patients, including those with extratemporal electroclinical findings, may suggest that the hippocampal atrophy is caused by repetitive seizures from the porencephaly; however, we did not find a correlation between severity of hippocampal volume loss and duration of epilepsy, nor was there a correlation between hippocampal volume loss and frequency of seizures. This suggests that hippocampal atrophy is unlikely to reflect progressive hippocampal damage resulting from propagation of partial seizures into the hippocampus.

A more likely mechanism to explain the dual pa-

TABLE 2: Data from control subjects used to calculate normalized volumes

Age Group, y	Mean, mm^3 (2 SD)				Cranial Volume, mean
	R Amygdala	L Amygdala	R Hippocampal Formation	L Hippocampal Formation	
25–38	2.44 (0.40)	2.32 (0.40)	3.96 (0.54)	3.63 (0.42)	1121.88
9–15	1.87 (0.32)	1.77 (0.52)	3.20 (0.30)	2.97 (0.22)	1057.00
3–6	1.74 (0.84)	1.78 (0.84)	3.17 (0.74)	2.89 (0.74)	877.71

TABLE 3: Qualitative and quantitative analysis of mesial temporal structures in the patients

Patient	Qualitative Analysis	Volumetric Measurements, mm^3			
		R Amygdala	L Amygdala	R Hippocampal Formation	L Hippocampal Formation
1	No visually detected AM-HF abnormality	2.54	1.81*	3.82	3.05*
2	L HF atrophy	2.49	1.39*	4.44	3.0*
3	R HF atrophy and T2 hyperintensity on FLAIR	1.88	2.65	1.4*	2.09*
4	R HF atrophy and T2 hyperintensity on FLAIR	1.89*	2.57	2.71*	3.39
5	R HF atrophy and T2 hyperintensity on FLAIR	2.35	2.65	3.79	3.98
6	R HF atrophy and T2 hyperintensity on FLAIR	1.23*	2.2	1.79*	2.73*
7	L HF atrophy	2.08	2.12	3.41*	3.13*
8	R HF atrophy	0.59*	2.44	2.5*	3.96
9	R HF atrophy	1.99*	2.11	3.3*	3.76
10	R HF atrophy and T2 hyperintensity on FLAIR	1.81*	2.17	2.77*	4.18
11	L HF atrophy and T2 hyperintensity on FLAIR	2.33	2.27	4.29	2.28*
12	L HF atrophy and T2 hyperintensity on FLAIR	2.57	2.45	4.92	2.73*
13	R HF T2 hyperintensity on FLAIR	0.96*	1.19*	1.77*	2.36*
14	No visually detected AM-HF abnormality	2.0*	1.98	3.23*	2.62*
15	L HF atrophy and T2 hyperintensity on FLAIR	2.28	2.26	2.42*	2.73*
16	L HF atrophy	1.18	0.47*	2.7	0.56*
17	Bilateral asymmetrical HF atrophy	1.78*	1.61*	3.21*	2.27*
18	No visually detected AM-HF abnormality	1.66*	1.86*	2.22*	2.57*
19	L HF T2 hyperintensity on FLAIR	2.06	2.06	3.69	2.17*
20	Bilateral symmetrical HF atrophy and T2 hyperintensity	1.79	1.77	2.59*	2.35*
21	L HF atrophy and T2 hyperintensity on FLAIR	1.17	1.08	2.33*	1.58*
22	R HF atrophy and T2 hyperintensity on FLAIR	2.14	2.26	2.88*	3.38

Note.—AM indicates amygdala; HF, hippocampal formation; and FLAIR, fluid-attenuated inversion recovery.

* Abnormal volumes, defined as less than 2 SD below mean for control group in corresponding age category.

thology is a common ischemic pathogenesis for the two lesions. The cause of mesial temporal sclerosis is unclear. In contrast, an ischemic mechanism for the pathogenesis of porencephaly is well established. This condition is usually caused by prenatal or perinatal cerebral vascular occlusion (16–18). Perinatal occlusion of the posterior cerebral artery has been previously reported in a small series of patients with temporal lobe epilepsy and porencephaly (19). The posterior cerebral artery supplies the occipital and part of the parietal lobe and the inferomesial and lateral areas of the temporal lobe, as well as Ammon's horn and part of the parahippocampal gyrus (20). The hippocampus and temporal lobe lie in a watershed area supplied mainly by the posterior cerebral and anterior choroidal arteries (20, 21). Therefore, either an arterial thrombosis or a drop in blood pressure in boundary zones between two areas of arterial supply can cause ischemic damage to the hippocampus. The same mechanism can cause tissue necrosis and cavitation, resulting in porencephaly.

Diaschisis is another mechanism that can explain the dual pathology and the high frequency of bilateral amygdalar and hippocampal atrophy. This term was used by von Monakow to describe remote effects after central nervous system injury, such as cerebral infarction (22, 23). Since then, different types of diaschisis have been recognized, including effects on the ipsilateral cerebral hemisphere and the contralateral hemisphere or transhemispheric diaschisis (23). The changes associated with diaschisis may involve interruption of hemispheric connections by the infarct causing deafferentation and transneural metabolic depression, impaired resting blood flow, or alteration in evoked electrophysiological activity in the remote ipsilateral or contralateral hemisphere (22–24). In humans, cerebral blood flow has been reported to be decreased contralateral to the infarction 1 to 2 weeks after onset of the lesion (25). Thus, either diaschisis following prenatal or perinatal cerebral vascular occlusion or watershed ischemia in the mesial temporal regions may lead to damage to the ipsilateral or contralateral amygdala-hippocampal formation.

Conclusion

This study provides evidence that widespread structural damage in the mesial temporal structures exists in patients with congenital porencephaly and intractable seizures. This finding has important implications for surgical therapy. Our data also provide insight into the possible mechanisms involved in the genesis of dual pathology and seizures in patients with congenital porencephaly.

References

1. Claeys V, Deonna T, Chrzanowski R. **Congenital hemiplegia: the spectrum of lesions, a clinical and computerized tomographic study of 37 cases.** *Helv Paediatr Acta* 1983;38:439–455
2. Kotlarek F, Rodewig R, Brull D. **Computed tomographic findings in congenital hemiparesis in childhood and their relation to etiology and prognosis.** *Neuropediatrics* 1981;12:101–109
3. Cohen ME, Duffner PK. **Prognostic indicators in hemiparetic cerebral palsy.** *Ann Neurol* 1981;9:353–357
4. Molteni B, Oleari G, Fedrizzi E. **Relation between CT patterns, clinical findings and etiological factors in children born at term, affected by congenital hemiparesis.** *Neuropediatrics* 1987;18:75–80
5. Cendes F, Cook MJ, Watson C, et al. **Frequency and characteristics of dual pathology in patients with lesional epilepsy.** *Neurology* 1995;45:2058–2064
6. Cendes F, Andermann F, Gloor P, et al. **MRI volumetric measurement of amygdala and hippocampus in temporal lobe epilepsy.** *Neurology* 1993;43:719–725
7. Cook MJ, Fish DR, Shorvon SD, Straughan K, Stevens JM. **Hippocampal volumetric and morphometric studies in frontal and temporal lobe epilepsy.** *Brain* 1992;115:1001–1015
8. Jack CR, Sharborough FW, Twomey CK, et al. **Temporal lobe seizures: lateralization with MR volume measurements of the hippocampal formation.** *Radiology* 1990;175:423–429
9. Free SL, Bergin PS, Fish DR, Cook MJ, Shorvon SD, Stevens JM. **Proposed methods for normalization of hippocampal volumes measured with MR.** *AJNR Am J Neuroradiol* 1995;16:637–643
10. Free SL, Li LM, Fish DR, Shorvon SD, Stevens JM. **Bilateral hippocampal volume loss in patients with a history of encephalitis or meningitis.** *Epilepsia* 1996;37:400–405
11. Patten J. **The cerebral hemispheres, 2: vascular diseases.** In: *Neurological Differential Diagnosis.* New York, NY: Springer-Verlag; 1987:86–98
12. Jackson GD. **The diagnosis of hippocampal sclerosis: other techniques.** *Magn Reson Imaging* 1995;13:1081–1093
13. Watson C, Andermann F, Gloor P, et al. **Anatomic basis of amygdaloid and hippocampal volume measurement by magnetic resonance imaging.** *Neurology* 1992;42:1743–1750
14. Jack CR, Twomey CK, Zinsmeister AR, Sharbrough FW, Petersen RC, Cascino GD. **Anterior temporal lobes and hippocampal formations: normative volumetric measurements from MR images in young adults.** *Radiology* 1989;172:549–554
15. Cavazos JE, Sutula TP. **Progressive neuronal loss induced by kindling: a possible mechanism for mossy fibre synaptic reorganization and hippocampal sclerosis.** *Brain Res* 1990;527:1–6
16. Norman R, Urich H, Woods G. **The relationship between prenatal porencephaly and encephalomalacias of early life.** *J Ment Sci* 1958;104:758–771
17. Freeman JM, Gold AP. **Porencephaly simulating subdural hematoma in childhood: a clinical syndrome secondary to arterial occlusion.** *Am J Dis Child* 1964;107:327–336
18. Eisenstein VW, Taylor HK. **Porencephalic cyst: report of a case with arterial studies.** *Arch Neurol Psychiatry* 1941;45:1009
19. Remillard GM, Ethier R, Andermann F. **Temporal lobe epilepsy and perinatal occlusion of the posterior cerebral artery: a syndrome analogous to infantile hemiplegia and a demonstrable etiology in some patients with temporal lobe epilepsy.** *Neurology* 1974;24:1001–1009
20. Kaplan HA. **Anatomy and embryology of the arterial system of the forebrain: vascular diseases of the nervous system.** In: Vinken PJ, Bruyn FW, eds. *Handbook of Clinical Neurology, Part 1.* Amsterdam, the Netherlands: North Holland; 1972
21. Coceani F, Gloor P. **The distribution of the internal carotid circulation in the brain of the macaque monkey (Macaca mulatta).** *J Comp Neurol* 1966;128:419–429
22. Feeney DM, Baron JC. **Diaschisis.** *Stroke* 1986;17:817–830
23. Andrews RJ. **Transhemispheric diaschisis.** *Stroke* 1991;22:943–949
24. Meyer JS, Hata T, Imai A. **Clinical and experimental studies of diaschisis.** In: Wood JH, ed. *Cerebral Blood Flow: Physiologic and Clinical Aspects.* New York, NY: McGraw-Hill; 1987:481–502
25. Baron JC. **Pathophysiology of acute cerebral ischaemia: PET studies in humans.** *Cerebrovasc Dis* 1991;1(Suppl 1):22–31